Measurements of the band gap of ThF$_4$ by electron spectroscopy techniques

T. Gouder,[1] R. Eloirdi,[1] R. L. Martin,[2] M. Osipenko,[3] M. Giovannini,[3,4] and R. Caciuffo [1]

[1]*European Commission, Joint Research Centre (JRC), Postfach 2340, D-76125 Karlsruhe, Germany*
[2]*Theoretical Division, Los Alamos National Laboratory, Los Alamos, New Mexico 87545, USA*
[3]*Istituto Nazionale Fisica Nucleare, INFN, Sezione di Genova, I-16146 Genoa, Italy*
[4]*Department of Chemistry, University of Genova, Via Dodecaneso 31, I-16146 Genoa, Italy*

We present an experimental determination of the band gap of ThF$_4$ performed by two different techniques. The first measurement was performed by combining x-ray photoemission spectroscopy and bremsstrahlung isochromat spectroscopy. The second measurement exploited the position of the inelastic threshold in reflection electron energy loss spectroscopy. Both measurements gave compatible values of the band gap, with the average $\Delta E = 10.2(2)$ eV. This value was found to be in excellent agreement with theoretical calculations. The measured band gap is significantly larger than the ^{229m}Th excitation energy, making ThF$_4$ a possible candidate material for a solid-state nuclear clock based on the vacuum ultraviolet γ decay.

I. INTRODUCTION

Transitions between two different states of an atomic nucleus generally involve energies of several tens of keV and above. Only two exceptions are known. One is the lowest-lying nuclear excited state of the ^{235m}U isomer that has been observed at 76.74 ± 0.02 eV [1]. The second, very recently confirmed by direct experiments [2], is provided by the $J^{\pi} = 3/2^+$ band head of the $\frac{3}{2}^+$[631] rotational band of ^{229}Th, an isotope created by the α decay of ^{233}U. Early studies of the γ radiation emitted by ^{229}Th suggested that its first excited state occurs at low energy [3], within 7 eV of the $J^{\pi} = 5/2^+$ ground state at the 2σ level [4,5]. Further studies confirmed the existence of an isomeric ^{229m}Th state that could be accessible by vacuum ultraviolet (VUV) radiation. Several attempts to detect the isomeric deexcitation directly have been performed during the past 30 years (see Ref. [6] and references therein), constraining the isomeric state energy E_{is} between 6.3 and 18.6 eV [2]. High-precision γ-ray spectroscopy provides an isomeric state energy $E_{is} = 7.8 \pm 0.5$ eV [7]. A value $E_{is} = 8.28 \pm 0.17$ eV has been obtained more recently from spectroscopy measurements of the internal conversion electrons in neutral ^{229m}Th [8]. This value corresponds to a wavelength of 149.7 ± 3.1 nm for the radiation emitted following the magnetic-dipole transition to the ground state, which is in a range accessible by frequency upconversion of laser sources.

The existence of an excited nuclear state at such a low energy has stimulated enormous interest, because the possibility to excite a nuclear transition by state-of-the-art lasers opens the way to a variety of applications in both fundamental and applied research. The most obvious one is the development of a solid-state optical *nuclear clock* [9,10]. Such a device would outperform atomic clocks owing to an unparalleled systematic frequency shift suppression and a higher stability ensured by a reduced quantum projection noise [10,11]. A total fractional inaccuracy approaching 10^{-19}–10^{-20} has been predicted for the operation of an optical ^{229}Th clock [12]. This would enable substantial improvement in global timekeeping and positioning, and would provide a powerful tool for improving the constraints on the space and time variation of fundamental physical constants [13–16].

Active optical pumping into ^{229m}Th has recently been reported [17], but attempts to optically excite the nuclear isomer or to observe directly its radiative decay to the ground state have so far failed [18–22]. One of the leading proposals for measuring this transition involves embedding ^{229}Th into a solid-state crystal and probing the nucleus using a VUV laser or undulator radiation at a synchrotron light source [14,20]. In order to be a good candidate as a host matrix, the crystal should satisfy several requirements. First, the band gap must be greater than the VUV spectrum. This is necessary as the crystal must be transparent for the nucleus to be excited by the laser. Moreover, a band gap larger than the isomer energy is necessary to suppress the internal conversion channel [23,24]. Second, the crystal should accommodate the Th^{4+} oxidation state to minimize the inhomogeneous broadening of the fluorescence signal. Finally, the crystal should be able to host ^{229}Th in regular lattice positions, in order to minimize color center defects that could interfere with the isomeric transition. With these constraints, ThF$_4$ is an ideal compound, provided that its band gap is large enough [25].

II. EXPERIMENTAL DETAILS

ThF$_4$ crystallizes in the monoclinic system within the $C2/c$ (No. 15) space group. Its crystal structure was recently refined by x-ray and neutron diffraction measurements [26] and is
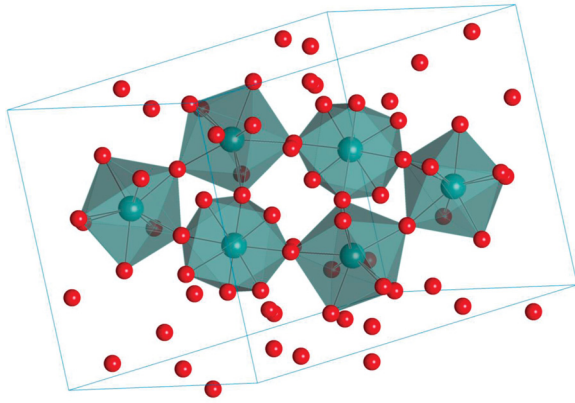

FIG. 1. Crystal structure of ThF_4, with thorium indicated in dark green and fluorine in red. Polyhedra indicate fluorine coordination around thorium atoms.
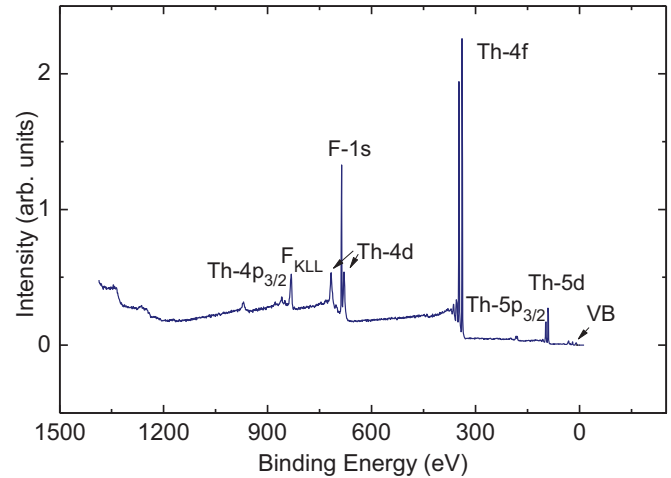

FIG. 2. Overview of the x-ray photoemission spectrum of ThF_4. Labels refer to the main XPS features in the explored binding energy range. Valence band (VB) spectra and the line corresponding to the Auger *KLL* process in fluorine (F_{KLL}) are also visible. Only thorium and fluorine lines were observed, showing that the measured sample was clean within the detection limit of XPS (about 1 at. %).

shown in Fig. 1. At room temperature, the lattice parameters are $a = 13.043(2)$ Å, $b = 11.010(2)$ Å, $c = 8.534(2)$ Å, and $\beta = 126.31(1)°$. The structure contains two Th and seven F inequivalent crystallographic sites, and consists of a three-dimensional network of corner-sharing ThF_8 square antiprisms.

To measure the band gap of ThF_4 we used two spectroscopic approaches: x-ray photoemission spectroscopy (XPS) combined with bremsstrahlung isochromat spectroscopy (BIS) and reflection electron energy loss spectroscopy (REELS).

Photoemission probes the valence (XPS) and the conduction (BIS) bands, and thus the gap separating them. REELS measures the excitation from the valence band (VB) to the conduction band (CB) by the energy loss of probing electrons upon reflection from the surface. Experiments were carried out on thin films of ThF_4 deposited on polycrystalline gold of 25 μm thickness. Gold was chosen because it does not react with ThF_4 and, even though AuF_4 exists, we have not observed any transfer of fluorine from the ThF_4 film to the Au substrate. There were two experimental challenges for the measurements: surface charging and surface decomposition. Surface charging is an issue in photoelectron spectroscopy, which involves either removal (XPS) or addition (BIS) of an electron. Buildup of surface charge shifts the binding energies in XPS and BIS (the shifts are generally different) and needs therefore to be quantified. In the case of thin films the shifts are expected to be small because the electrons can tunnel through the film to the metallic substrate. Surface decomposition is also an issue for spectroscopies involving irradiation with electrons (BIS and REELS). In particular, it is critical for BIS because of the long data acquisition time. As a consequence, we took precautions and paid special attention to avoid or monitor surface decomposition.

A. Thin-film deposition and characterization

Thin films were prepared by sublimation of ThF_4 starting material produced by reaction of $Th(NO_3)_4$ and HF in solution. The product was first dried by heating under air for 2 h at 373 K, then it was mounted as dry powder in the electron

beam crucible. The chamber was pumped down slowly ($\sim 10^{-6}$ mbar/min before baking) to favor gradual evaporation of residual water bound to ThF_4. Then the evaporator was gently heated to 393 K (~ 0.5 K/min) under ultrahigh vacuum (UHV) and kept at that temperature for 2 h. After 24 h of chamber baking, the electron beam was switched on and the crucible was further heated starting with 1 W heating power while monitoring pressure and gas composition by mass spectrometry. Besides the usual water (18 amu), CO (28 amu), and CO_2 (44 amu), during the outgassing phase we observed peaks at 30 amu (NO) and 46 amu (NO_2) resulting from the evaporation and decomposition of HNO_3. Residual $Th(NO_3)_4$ and ThO_2 have a higher sublimation temperature than ThF_4. Therefore, even in the presence of these impurities, clean ThF_4 films can be produced by sublimation. XPS overview scans confirmed the cleanliness of the films (within 1 at. %), as shown in Fig. 2.

For sublimation, we used the AFM3 electron beam evaporator from FOCUS. The evaporant was placed in a tungsten crucible of 250 mm^3 and a heating power of 15 W was applied. The evaporation rate was monitored by the ion flux of the evaporant (being partially ionized by the *e*-beam), which was a simple way for monitoring and regulating the sputtering rate and ensuring reproducible film thicknesses. We worked at an acceleration voltage of 1 kV, with a sample/crucible distance of 200 mm, and a total evaporation amount of 10 mA s (flux $\times$ time). As ThF_4 did not decompose during evaporation, clean stoichiometric thin films were easily obtained.

Because of the long acquisition time (typically ~ 2 h), some degree of surface degradation does occur during BIS measurements. Indeed, under electron beam exposure at measuring conditions ThF_4 eventually turned black. To avoid it, the sample was scanned under the electron beam and a large number of measurement spots (10×10) was taken, with an individual run acquisition time of 30 s. Under these conditions, no color change was observed. The measurement

sequence was repeated twice, providing equivalent spectra. As a further check of the sample surface integrity, Th 4f core-level spectra were collected before and after the BIS run. The latter exhibited weak, steplike features at a binding energy (BE) lower than the main 4f lines. This is typical for reduced atoms in buried layers, with photoelectrons losing energy by inelastic scattering while traveling through the solid. The results therefore suggest that ThF$_4$ decomposition occurs in deeper layers, probably at the interface with Au, with F atoms diffusing in the substrate and Th-Au intermetallic phases forming at the interface. A semiquantitative analysis gives an amount of reduced Th at the level of ∼2 at. %.

B. Data acquisition and electron energy calibration

High-resolution (∼0.5 eV) x-ray photoemission spectroscopy (XPS) measurements were performed using a Phoibos 150 hemispherical analyzer. Al $K\alpha$ ($E = 1486.6$ eV) radiation was produced by a XRC-1000 microfocus source, equipped with a monochromator and operating at 120 W. The background pressure in the analysis chamber was 2×10^{-10} mbar. The spectrometer was calibrated using the Au $4f_{7/2}$ line (83.9 eV) and Cu $2p_{3/2}$ (932.7 eV) of metallic gold and copper standards. Photoemission spectra were taken at room temperature.

Electrons for bremsstrahlung isochromat spectroscopy (BIS) were obtained by a SPECS EQ 22/35 electron source. The gun was equipped with a tungsten filament coated with BaO to improve the energy resolution of the electrons to about 0.4 eV full width at half maximum. The actual resolution of the BIS spectra was worse because of lifetime and solid-state broadening effects.

Reflection electron energy loss spectroscopy (REELS) spectra were obtained using 1–1.4 keV electrons from the same electron gun. Reflected electron energies were analyzed with the Phoibos 150 hemispherical analyzer. Auger emission spectra were excited either by x rays (XAES) or primary electrons (AES). Comparison of their energy allowed evaluation of different surface charging in XPS and BIS.

The electron energy calibration has been performed by measuring XPS and BIS spectra around the Fermi level of a gold reference standard. BIS data have been collected with a kinetic energy at the Fermi level $E_{\mathrm{kin}}(E_F) = 1484.2$ eV. We assumed that the Fermi energy corresponded to the midpoint of the intensity jump in the spectra, which was determined by fitting three straight lines to the experimental data, as shown in Fig. 3. Due to an offset of the analyzer, for the XPS spectrum we found a shift of about $-0.07(3)$ eV with respect to zero energy. In the BIS case, the energy shift due to an offset of the electron gun was ∼ $+0.47(9)$ eV. In insulating ThF$_4$, the Fermi level lies in the gap between valence and conduction bands, and therefore there is no signal around it in photoemission spectra. However, provided that surface charging does not take place, the binding energy corrections are the same as for the metal standard. We will show below that this is indeed the case in our study. Accordingly, the XPS spectra shown below for ThF$_4$ have been shifted by 0.07 eV to higher BE, while the BIS spectra have been shifted by 0.47 eV to lower BE. The calibration was regularly repeated during the
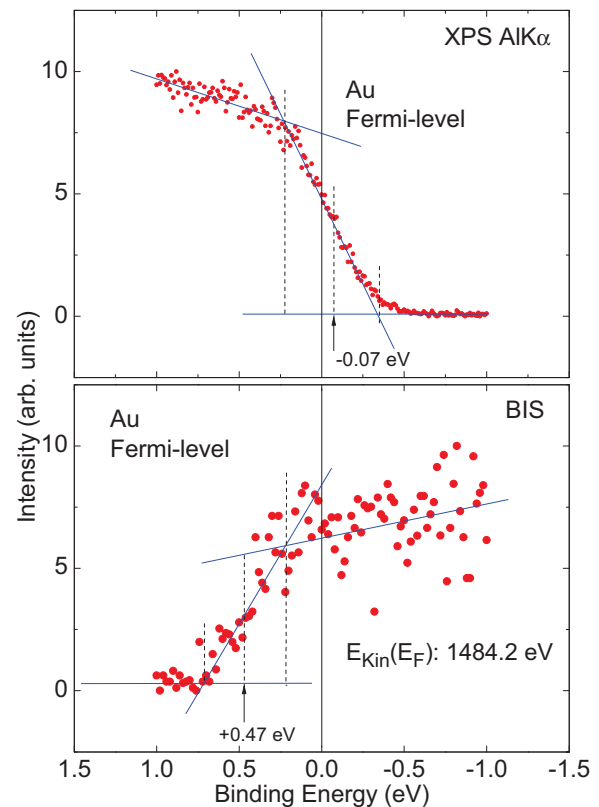

FIG. 3. Energy calibration in x-ray photoemission (top panel) and bremsstrahlung isochromat spectroscopy (bottom panel). Spectra were collected around the Fermi level of a gold standard using Al $K\alpha$ radiation ($E = 1486.6$ eV) for XPS and electrons with kinetic energy $E_{\mathrm{kin}} = 1484.2$ eV (at the Fermi level) for BIS. Energy shifts of ∼ $-0.07(3)$ eV in XPS and ∼ $+0.47(9)$ eV in BIS were observed, due to the analyzer and electron-gun offsets, respectively.

different data acquisition steps, with consistent results for the observed shifts.

III. RESULTS AND DISCUSSION

The Th 4f core-level spectra obtained by XPS at room temperature are shown in Fig. 4. The two strong peaks correspond to the $4f_{5/2}$ and $4f_{7/2}$ excitations at 347.3 and 338.0 eV binding energy (BE), respectively. The observed BEs are higher than literature data (346.3 and 337.1 eV, respectively) [27]. This can be attributed to slight surface charging for our sample or to slightly incorrect charge neutralization in literature. In Ref. [27] measurements were done on a bulk sample using surface charge corrections, a procedure that often introduces systematic errors. Working with thin films reduces charging effects because of residual electrical conductivity and electron tunneling. However, since the film we used was rather thick (roughly 25 nm, as deduced from the damping of the substrate Au 4f line), we repeated the core-level XPS measurements on films with different thicknesses, obtaining in all cases the same binding energy. This points against surface charging. Another argument to exclude surface charge effects is that the fluorine KLL Auger lines are observed at the
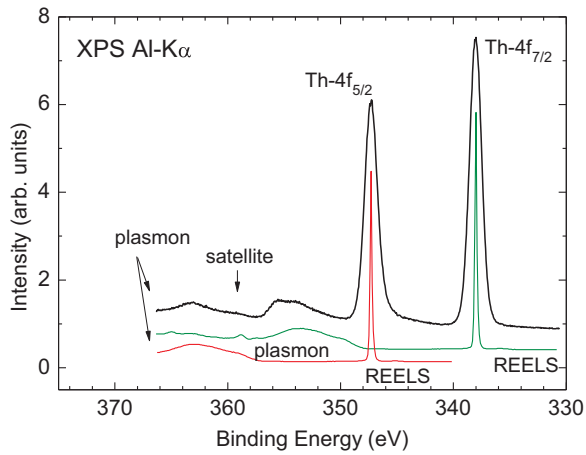
FIG. 4. Thorium $4f$ core-level x-ray photoemission spectrum in ThF_4, collected using monochromatized Al $K\alpha$ radiation ($E = 1486.6$ eV) with an energy resolution of $\sim$0.5 eV at the Au $4f_{7/2}$ peak. The binding energy (BE) is measured relative to the Fermi level. Dissipation features due to plasmon excitations are revealed by reflection electron energy loss spectra (REELS) collected with a primary electron energy corresponding to the kinetic energy of the Th $4f_{7/2}$ (green) and $4f_{5/2}$ (red) lines after Al $K\alpha$ excitation.

FIG. 5. KLL Auger spectrum of fluorine in ThF_4, excited by primary electrons (AES, red line) or by x ray (XAES, blue line). The characteristic ^1P (858.8 eV), ^3P (850.5 eV), ^1S (834.9 eV), and ^1D (831.8 eV) lines are clearly visible. The data sets shown at the bottom are reference spectra taken with improved statistics, whereas the spectra shown at the top have been collected simultaneously with the valence band (VB) and the BIS spectra. An arbitrary shift has been applied on the vertical scale for visual convenience.

same energy both in the XPS (Fig. 2) and in the BIS spectra (see below).

The high BE satellite is a superposition of a charge transfer satellite (Th $5f \rightarrow$ F $2p$ transition in the final state) and loss features (plasmon). The latter are visualized by a REELS spectrum (Fig. 4) taking as the primary electron energy 1145 eV (roughly corresponding to the Th $4f$ lines kinetic energy E_{kin} after Al $K\alpha$ excitation).

For insulators, the Fermi level does not align with the spectrometer. Therefore, in the presence of surface charge, it can no longer be used as a reference. In XPS, surface charge is due to photoemission of electrons, whereas in BIS it is due to secondary electron emission (and is generally higher than in XPS). The presence of surface charge can be assessed by measuring the fluorine KLL Auger emission line, which is observable both in XPS (excited by x ray) and BIS (excited by primary electrons). This is an internal deexcitation with a fixed characteristic energy that depends uniquely from the electronic structure of the excited atom. Any difference in its energy in XPS and BIS therefore signals the presence of surface charge.

Figure 5 compares x-ray induced (XAES) and electron-induced Auger spectra (AES) obtained for the investigated ThF_4 thin films. The two spectra at the bottom of the figure have been recorded over an energy range including the characteristic ^1P and ^1D fluorine KLL emission lines. The shift in energy between the pair of spectra at the bottom indicates an alteration of the surface composition during the AES run. The two curves at the top of the figure are, instead, the spectra taken during the measurements of the BIS and of the valence band (VB) XPS spectra (with a shorter acquisition time and decreased electron-gun intensity to avoid decomposition). Within measurement uncertainties of about 0.5 eV, the emission lines are observed at the same energy in the VB and
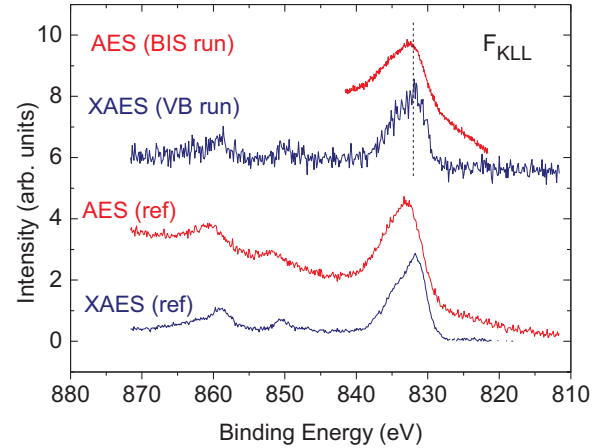
BIS spectra, showing that surface charge effects are negligible and no supplementary energy shifts are required.

Figure 6 shows the combined XPS-BIS spectra of ThF_4. A large valence-band peak appears between 13 and 8 eV binding energy. The cutoff energy is about 8 eV. The conduction band appears as a considerably narrower peak between -3 and -6 eV binding energy. The band gap, determined as the energy difference between the onset point of the intensity in the valence and conduction bands, is $\Delta E = 10.3(2)$ eV. This is about 2 eV larger than the isomer excitation energy expected for ^{229}Th, showing that ThF_4 is a suitable candidate material for directly observing the radiative transition in ^{229}Th-doped crystals and for the realization of an optical nuclear clock.
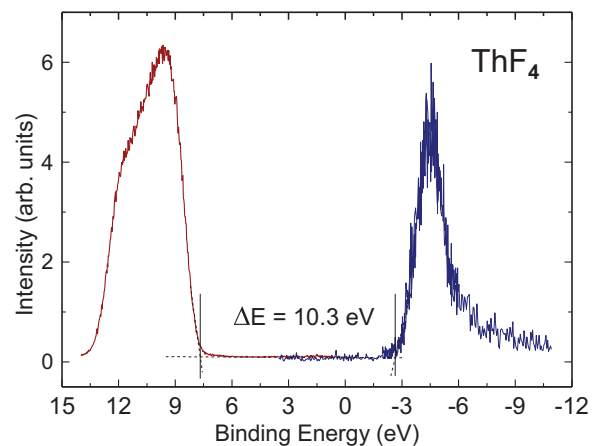

FIG. 6. X-ray photoemission (red) and bremsstrahlung isochromat (blue) spectra of ThF_4 showing a band gap of $\Delta E = 10.3(2)$ eV. Fermi-level calibration and energy shift due to surface charge effects have been applied as discussed in the text.
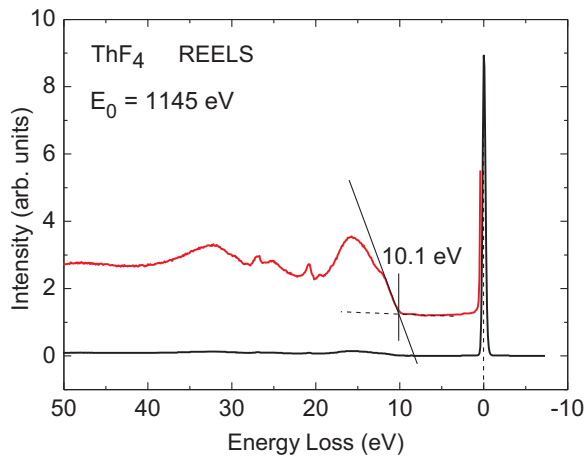
FIG. 7. Reflection electron energy loss spectroscopy (REELS) results for the ThF$_4$ thin film collected at a primary electron energy $E_0 = 1145$ eV (black curve). The red curve shows the same data with intensity multiplied by a factor 20. A gap $\Delta E = 10.1(2)$ eV is estimated from the onset values of the loss-signal spectrum.

To verify the validity of the result obtained for the band gap in ThF$_4$, we have performed reflection electron energy loss spectroscopy (REELS) measurements on a film similar to the one used for the XPS/BIS experiments.

REELS measurements imply resolving the change in kinetic energy that occurs when the collision between electrons and the sample surface is inelastic. Using electron beams with energy of the order of 1 keV, the technique probes a surface layer of about 10 nm thickness and provides a straightforward way to obtain the band gap of a dielectric thin film. Indeed, the band-gap value corresponds simply to the onset due to electron-hole excitation. Figure 7 shows the REELS data obtained for ThF$_4$ using primary electrons with a kinetic energy $E_0 = 1145$ eV. The band gap is given by the energy loss value corresponding to the intersection of two linear fits, one to the onset of the loss-signal spectrum and one to the background level [28,29]. Following this procedure, we obtain a value $\Delta E = 10.1(2)$ eV, in excellent agreement with the one obtained by direct and inverse photoemission spectroscopy.

Previously published electronic structure calculations based on the many-body Green's function (G$_0$W$_0$) approach [25] predict a gap value of 10.1 eV, in excellent agreement with the experiments. The 3 eV conduction bandwidth measured is also in good agreement with the previous screened hybrid density functional [Heyd-Scuseria-Ernzerhof (HSE)]

theory and G$_0$W$_0$ calculations [25]. Interestingly, this bandwidth is slightly narrower than that observed in BIS spectra that we recorded for thin films of ThO$_2$ ($\sim$4 eV) and more than a factor of 2 smaller than the one we measured for UF$_4$ thin films ($\sim$8 eV), in agreement with earlier observations on these compounds by other techniques [30,31]. In both ThO$_2$ and ThF$_4$ the conduction band is formally f^0 and completely empty. Its bandwidth reflects a one-electron origin: hybridization effects and the spin-orbit splitting. Because the O $2p$ levels lie much closer in energy to the Th $5f$, one expects a more covalent, less ionic interaction in ThO$_2$, leading to a larger conduction bandwidth. This difference in ligand and metal orbital energies are also reflected in the gap itself, which is a ligand-metal charge transfer transition in both cases. On the other hand, this simple picture is complicated in later members of the actinide series where the ground state formally occupies f orbitals. In UF$_4$ the ground state is formally f^2, and additional final-state multiplet effects can contribute to the width.

IV. CONCLUSIONS

In summary, the band gap of ThF$_4$ was measured by two different electron spectroscopy techniques. The first measurement was performed using the difference between x-ray photoemission spectroscopy and bremsstrahlung isochromat spectroscopy. The second measurement exploited the position of inelastic threshold in reflection electron energy loss spectroscopy. Both measurements gave compatible values of the band gap, with the average $\Delta E = 10.2(2)$ eV. This value was found to be in excellent agreement with first-principles electronic structure calculations. The measured band gap is significantly larger than the ^{229m}Th excitation energy (7.5 eV from indirect measurements and 8.3 eV from direct measurements), making ThF$_4$ a possible candidate material for a solid-state nuclear clock. This allows us to suppress the dominant internal conversion decay channel, giving the possibility to design a simpler feedback detection system. To maximize the signal-to-background ratio, the density of possible intermediate levels due to crystal border effects or structure defects have to be reduced. To test this idea, a technique for the growth of a single-crystal ThF$_4$ film has to be developed along with a narrow bandwidth, variable wavelength VUV laser comb.

[1] F. Ponce, E. Swanberg, J. Burke, R. Henderson, and S. Friedrich, Phys. Rev. C **97**, 054310 (2018).

[2] L. von der Wense, B. Seiferle, M. Laatiaoui, J. B. Neumayr, H.-J. Maier, H.-F. Wirth, C. Mokry, J. Runke, K. Eberhardt, C. E. Düllmann *et al.*, Nature (London) **533**, 47 (2016).

[3] L. A. Kroger and C. W. Reich, Nucl. Phys. A **259**, 29 (1976).

[4] C. W. Reich and R. G. Helmer, Phys. Rev. Lett. **64**, 271 (1990).

[5] R. G. Helmer and C. W. Reich, Phys. Rev. C **49**, 1845 (1994).

[6] E. Peik and M. Okhapkin, C. R. Phys. **16**, 516 (2015).

[7] B. R. Beck, J. A. Becker, P. Beiersdorfer, G. V. Brown, K. J. Moody, J. B. Wilhelmy, F. S. Porter, C. A. Kilbourne, and R. L. Kelley, Phys. Rev. Lett. **98**, 142501 (2007).

[8] B. Seiferle, L. von der Wense, P. V. Bilous, I. Amersdorffer, C. Lemell, F. Libisch, S. Stellmer, T. Schumm, C. E. Düllmann, A. Pálffy *et al.*, Nature (London) **573**, 243 (2019).

[9] E. V. Tkalya, V. O. Varlamov, V. V. Lomonosov, and S. A. Nikulin, Phys. Scr. **53**, 296 (1996).

[10] E. Peik and C. Tamm, Europhys. Lett. **61**, 181 (2003).

[11] C. J. Campbell, A. G. Radnaev, A. Kuzmich, V. A. Dzuba, V. V. Flambaum, and A. Derevianko, Phys. Rev. Lett. **108**, 120802 (2012).

[12] G. A. Kazakov, A. N. Litvinov, V. I. Romanenko, L. P. Yatsenko, A. V. Romanenko, M. Schreitl, G. Winkler, and T. Schumm, New J. Phys. **14**, 083019 (2012).

[13] L. Cacciapuoti and C. Salomon, Eur. Phys. J. Spec. Top. **172**, 57 (2009).

[14] W. G. Rellergert, D. DeMille, R. R. Greco, M. P. Hehlen, J. R. Torgerson, and E. R. Hudson, Phys. Rev. Lett. **104**, 200802 (2010).

[15] R. M. Godun, P. B. R. Nisbet-Jones, J. M. Jones, S. A. King, L. A. M. Johnson, H. S. Margolis, K. Szymaniec, S. N. Lea, K. Bongs, and P. Gill, Phys. Rev. Lett. **113**, 210801 (2014).

[16] N. Huntemann, B. Lipphardt, C. Tamm, V. Gerginov, S. Weyers, and E. Peik, Phys. Rev. Lett. **113**, 210802 (2014).

[17] T. Masuda *et al.*, arXiv:1902.04823.

[18] C. J. Campbell, A. G. Radnaev, and A. Kuzmich, Phys. Rev. Lett. **106**, 223001 (2011).

[19] O. A. Herrera-Sancho, N. Nemitz, M. V. Okhapkin, and E. Peik, Phys. Rev. A **88**, 012512 (2013).

[20] J. Jeet, C. Schneider, S. T. Sullivan, W. G. Rellergert, S. Mirzadeh, A. Cassanho, H. P. Jenssen, E. V. Tkalya, and E. R. Hudson, Phys. Rev. Lett. **114**, 253001 (2015).

[21] L. von der Wense, B. Seiferle, S. Stellmer, J. Weitenberg, G. Kazakov, A. Pálffy, and P. G. Thirolf, Phys. Rev. Lett. **119**, 132503 (2017).

[22] S. Stellmer, G. Kazakov, M. Schreitl, H. Kaser, M. Kolbe, and T. Schumm, Phys. Rev. A **97**, 062506 (2018).

[23] E. V. Tkalya, A. N. Zherikhin, and V. I. Zhudov, Phys. Rev. C **61**, 064308 (2000).

[24] E. V. Tkalya, J. Exp. Theor. Phys. Lett. **71**, 311 (2000).

[25] J. K. Ellis, X.-D. Wen, and R. L. Martin, Inorg. Chem. **53**, 6769 (2014).

[26] L. Martel, E. Capelli, M. Body, M. Klipfel, O. Beneš, L. Maksoud, P. E. Raison, E. Suard, L. Visscher, C. Bessada *et al.*, Inorg. Chem. **57**, 15350 (2018).

[27] G. C. Allen, P. M. Tucker, and J. W. Tyler, Philos. Mag. B **48**, 63 (1983).

[28] H. Jin, S. K. Oh, Y. J. Cho, H. J. Kang, and S. Tougaard, J. Appl. Phys. **102**, 053709 (2007).

[29] D. Tahir, H. L. Kwon, H. C. Shin, S. K. Oh, H. J. Kang, S. Heo, J. G. Chung, J. C. Lee, and S. Tougaard, J. Phys. D: Appl. Phys. **43**, 255301 (2010).

[30] S. M. Butorin, K. O. Kvashnina, J. R. Vegelius, D. Meyer, and D. K. Shuh, Proc. Natl. Acad. Sci. USA **113**, 8093 (2016).

[31] J. G. Tobin, S. W. Yu, R. Qiao, W. L. Yang, and D. K. Shuh, J. Vac. Sci. Technol. A **36**, 061403 (2018).